Planck intermediate results. LIV. Polarized dust foregrounds

Planck Collaboration *

F. Boulanger (Ecole Normale Supérieure, Paris)
T. Ghosh (NISER, Bhubaneswar)

Statistical and frequency characterization of polarized foregrounds down to the lowest multipoles using the latest (PR3-2017) Planck maps

- Dust power spectra (follow-up of Planck Inter. XXX)
- Spectral energy distribution of Galactic polarized foregrounds (follow-up of Planck Inter. XXII)
- Frequency correlation of dust polarization maps (follow-up of Planck Inter. L)

➡ Data inputs for astrophysical and statistical modelling of polarized foregrounds to optimize component separation and assess uncertainties

Methodology

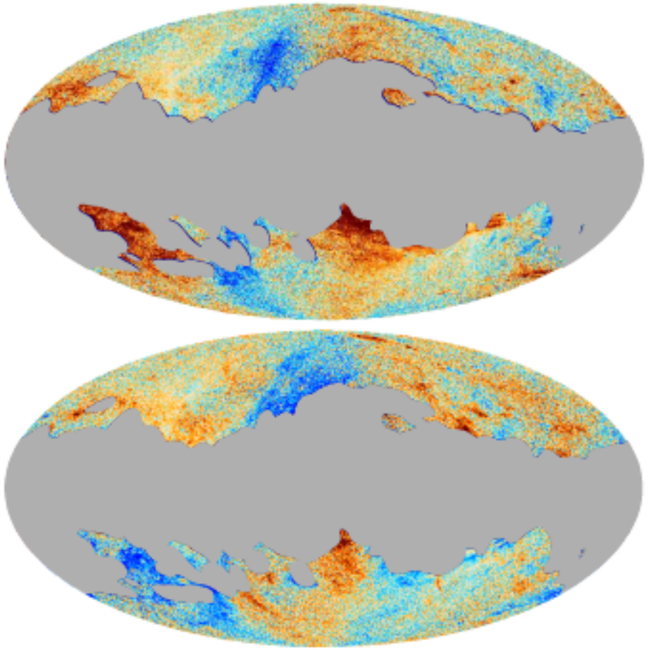

Q and U maps at 353 GHz

XPOL
pseudo-C_ℓ estimator
based on **XSPECT**
[Tristram et al. 2005]

Corrects for incomplete sky coverage, pixel and beam window functions

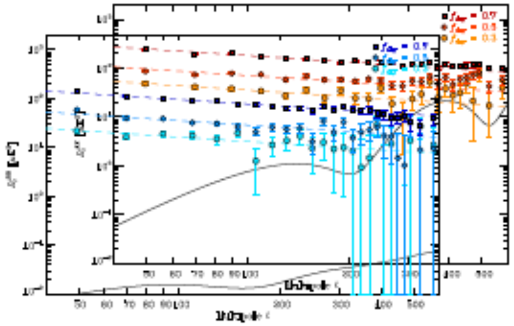

Angular power spectra

- Data analysis performed in harmonics space, within multipole bins, using cross spectra of polarization Planck (HFI & 30 GHz LFI) and WMAP (23 & 33 GHz) data. Spectra at a given frequency are computed from *independent* data subsets.
- CMB subtracted in power spectra using the Planck-2015 ΛCDM model
- Uncertainties from end-to-end (E2E) simulations include data noise and residual systematics

Sky regions

- Maks built from the smoothed (10°) dust intensity map at 857 GHz
- CO emitting regions and polarized point sources are masked
- Apodization (5°)

➡ Six nested sky regions with sky from 24 to 72% (LR24 to LR72) as in PXXX

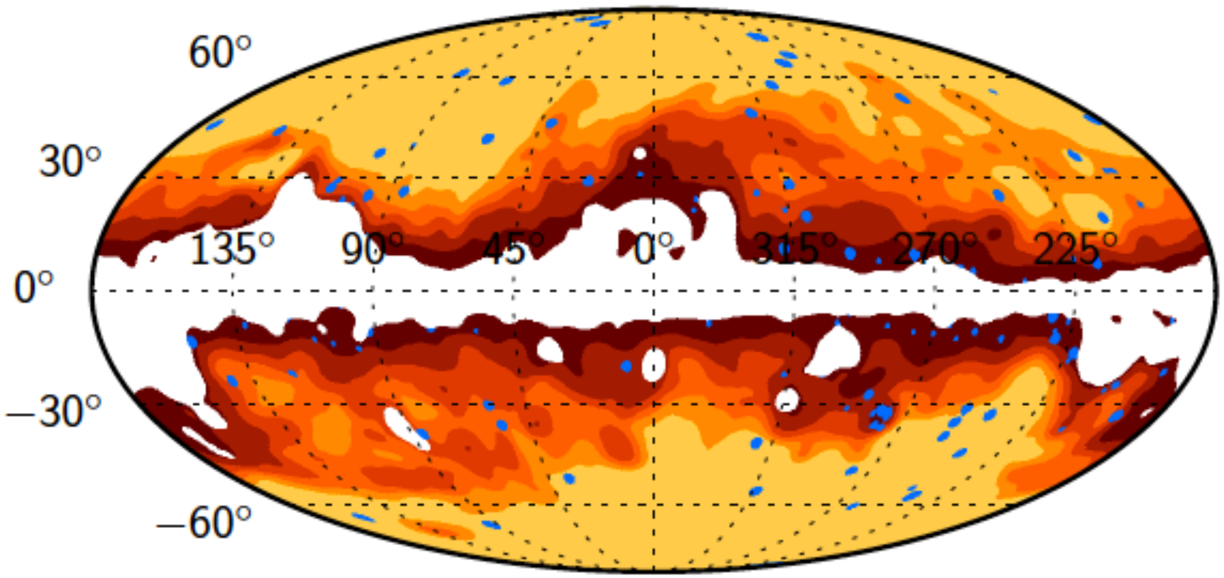

Data uncertainties

One realization of Q_{353}, U_{353}

error-maps from E2E simulations

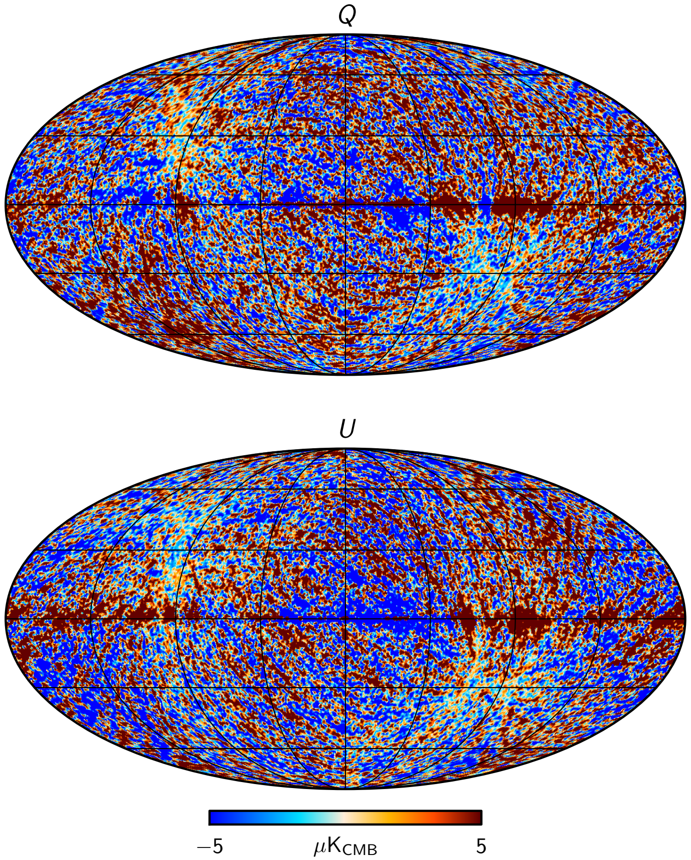

Half-difference half-mission maps

Error maps from E2E simulations

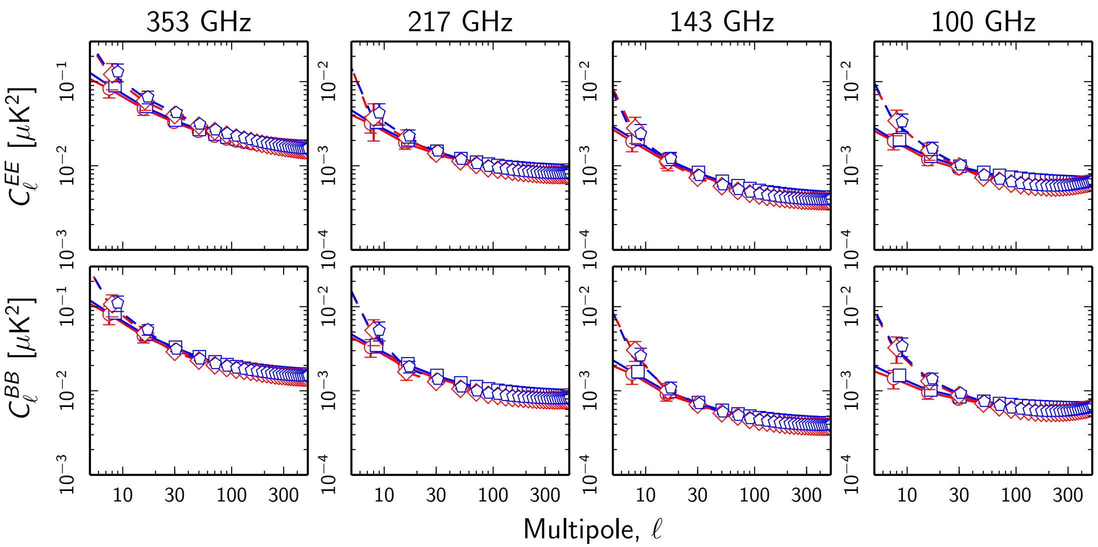

- E2E simulations (300 realizations) include known systematics and data noise
- Systematic uncertainty from polarization efficiencies

Dust TE, EE and BB power spectra

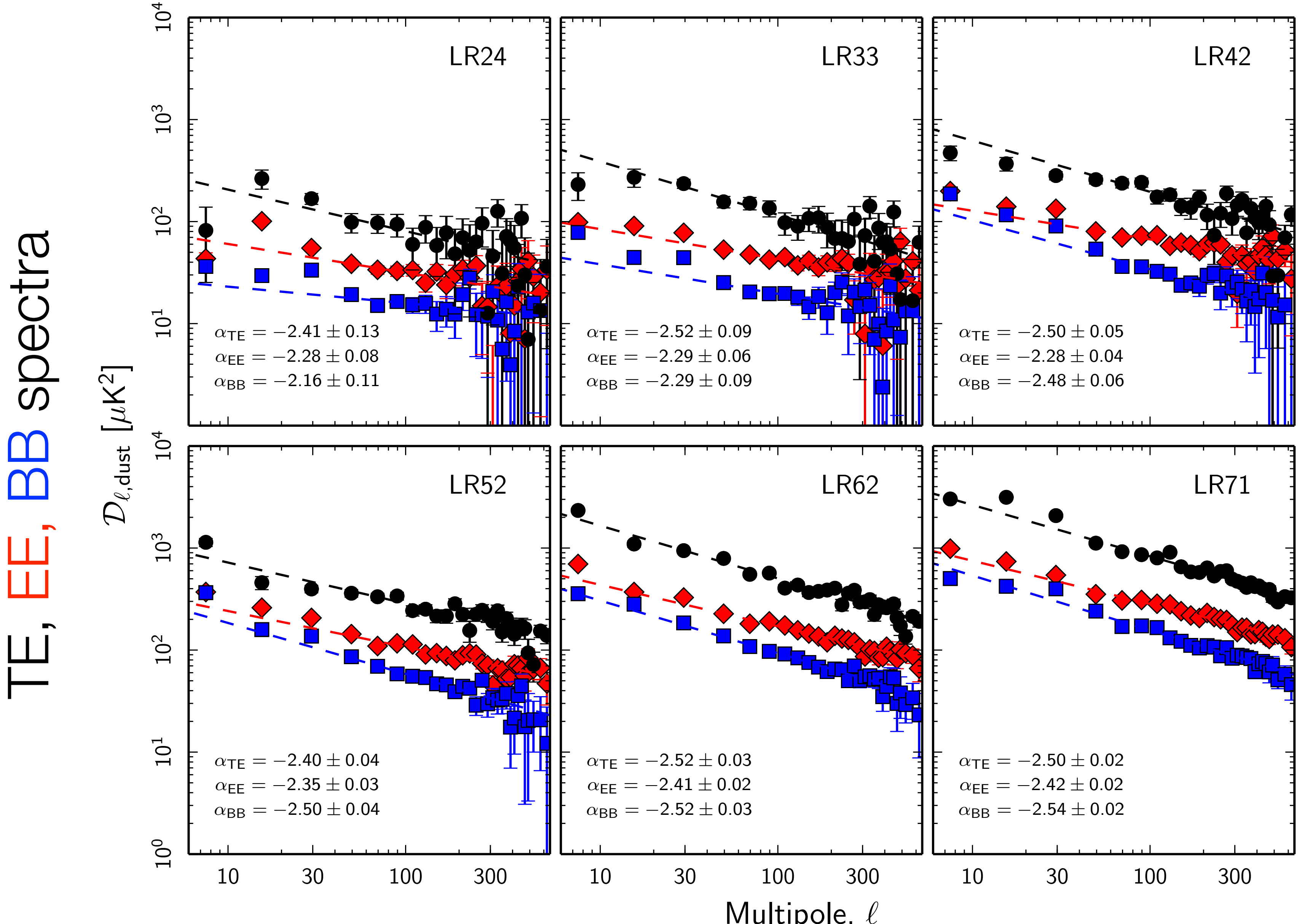

Power-law fits

$$D_\ell^{XY} \equiv A^{XY}(\ell/80)^{\alpha_{XY}+2} \text{ for } 40 < \ell < 600$$

$$< A^{BB}/A^{EE} >= 0.52 \pm 0.01$$

$$< \alpha_{EE} >= -2.38 \pm 0.02$$

$$< \alpha_{BB} >= -2.51 \pm 0.02$$

$$< \alpha_{TE} >= -2.49 \pm 0.02$$

- We find slightly different exponents for EE and BB
- No systematic reduction of the EE/BB power asymmetry at very low multipoles
- Large variations in the EE/BB ratio on the lowest ell-bin
- Spectra are not well fitted by a single power-law over the full multipole-range

➡ A model is required to interpret these results, in particular to model spectra and cosmic variance of dust polarization down to low multipoles.

➡ We are working on an update of the Vansyngel+2017 model

Scaling of BB power with dust total intensity

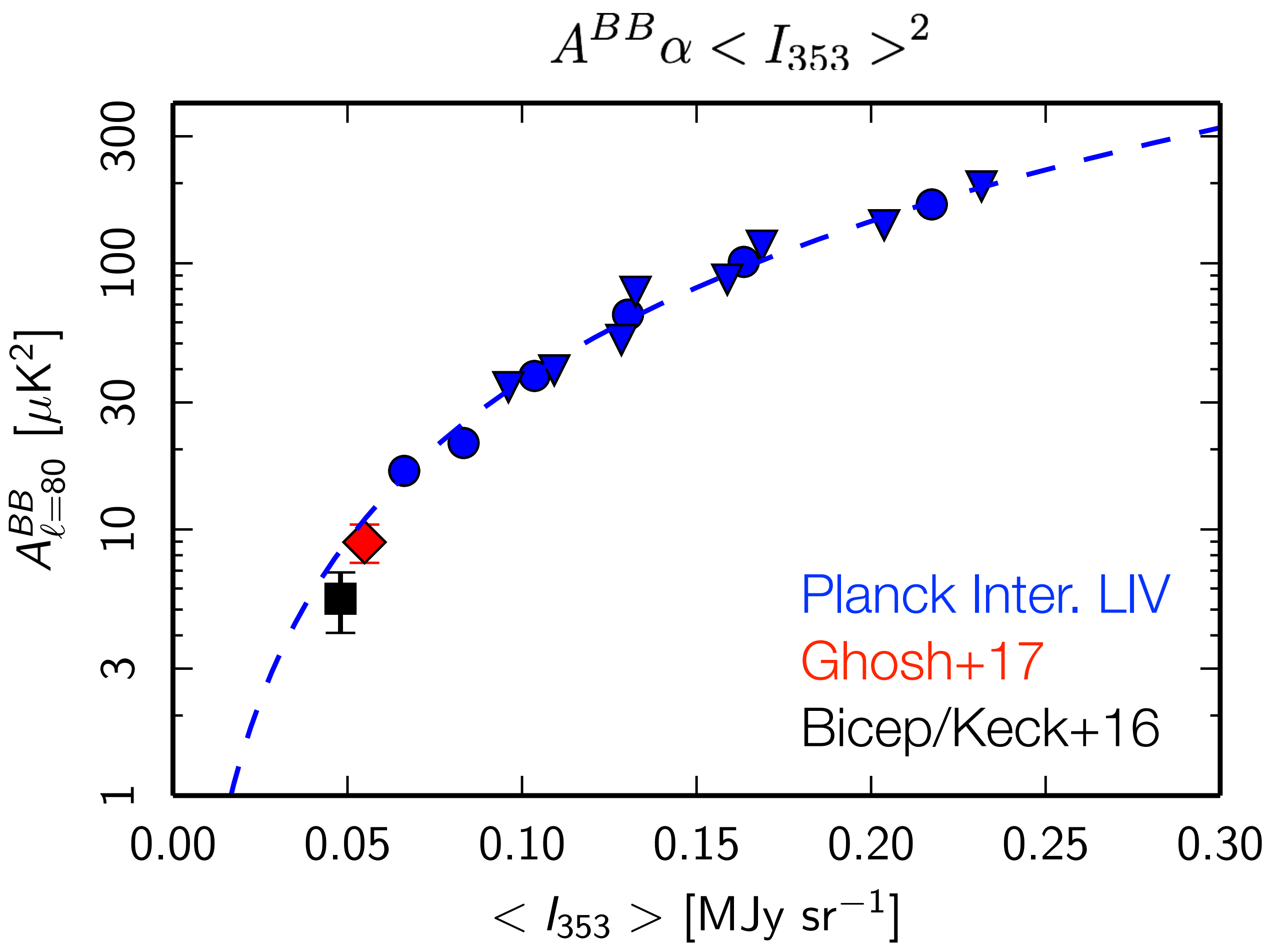

- B-mode dust power scales as the total dust intensity square
- Fit consistent with measurement for clean sky in the southern Galactic cap (fsky = 8.5%) in Ghosh+17
- Slightly above B-mode dust power derived from the cross-correlation with Planck for the Bicep/Keck field (fsky = 1%)

Dust TE correlation

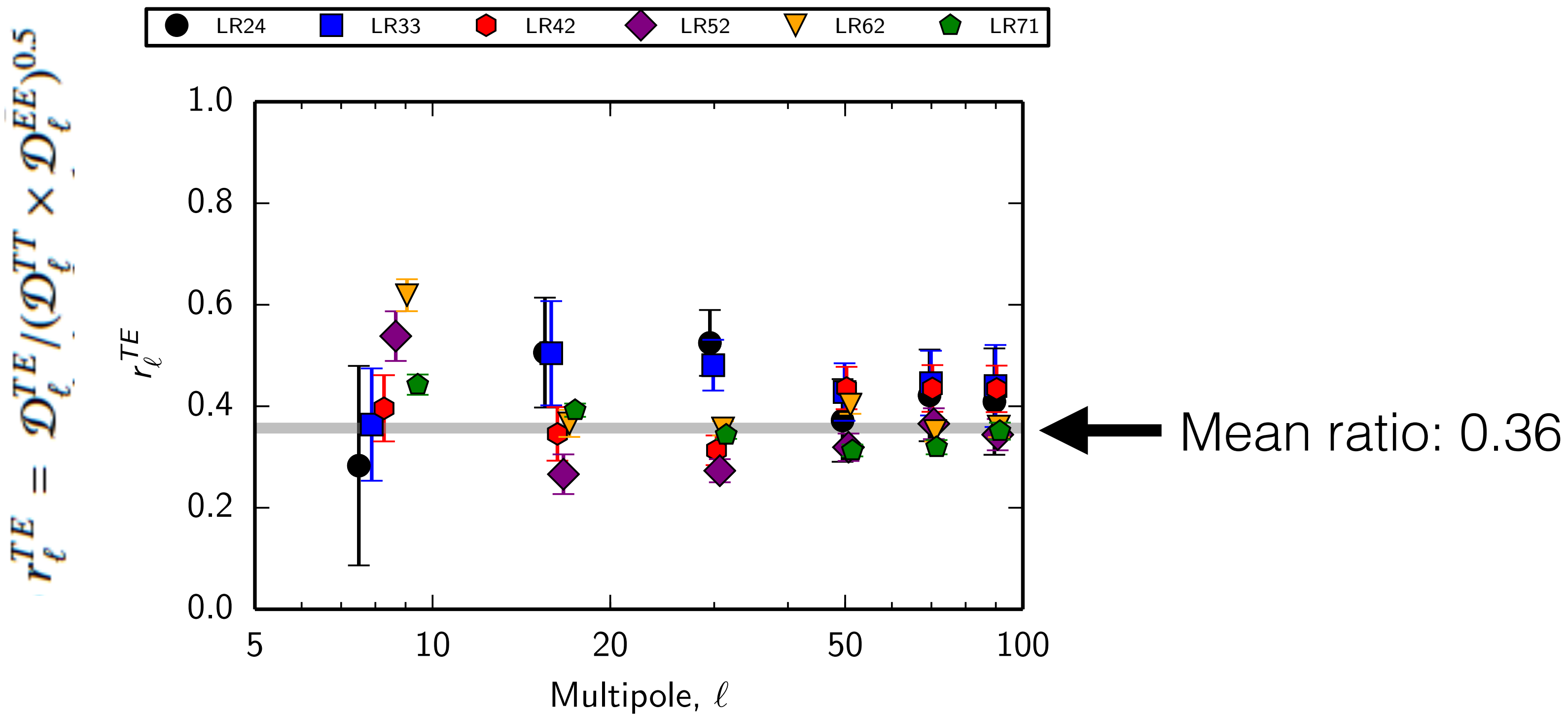

- The TE correlation extends to the lowest multipoles

➡ There is more to it than the alignment observed locally between the magnetic field and the filamentary structure of the ISM

➡ Symmetric variations of the mean orientation of the local magnetic field from the Galactic plane to the poles (follow-up model paper)

Frequency analysis of polarized foregrounds

Amplitude of EE/BB cross-spectra between frequencies $\boldsymbol{\nu}_1$ and $\boldsymbol{\nu}_2$:

Synchrotron

Dust

$$\mathcal{D}_\ell^{XX}(\nu_1 \times \nu_2) = A_s^{XX} \left(\frac{\nu_1 \nu_2}{30^2}\right)^{\beta_s} + A_d^{XX} \left(\frac{\nu_1 \nu_2}{353^2}\right)^{\beta_d - 2} \frac{B_{\nu_1}(T_d)}{B_{353}(T_d)} \frac{B_{\nu_2}(T_d)}{B_{353}(T_d)} + \rho^{XX}(A_s^{XX} A_d^{XX})^{0.5} \left[\left(\frac{\nu_1}{30}\right)^{\beta_s} \left(\frac{\nu_2}{353}\right)^{\beta_d - 2} \frac{B_{\nu_2}(T_d)}{B_{353}(T_d)} + \left(\frac{\nu_2}{30}\right)^{\beta_s} \left(\frac{\nu_1}{353}\right)^{\beta_d - 2} \frac{B_{\nu_1}(T_d)}{B_{353}(T_d)} \right],$$

Synchrotron x Dust

Same model as in Choi & Page (2015)

Five model parameters:

- The synchrotron and dust amplitudes A_s and A_d
- The two spectral indices β_s and β_d
- The dust/synchrotron polarization correlation parameter $\boldsymbol{\rho}$

→ Tuhin's talk

Dust and synchrotron power vs multipole

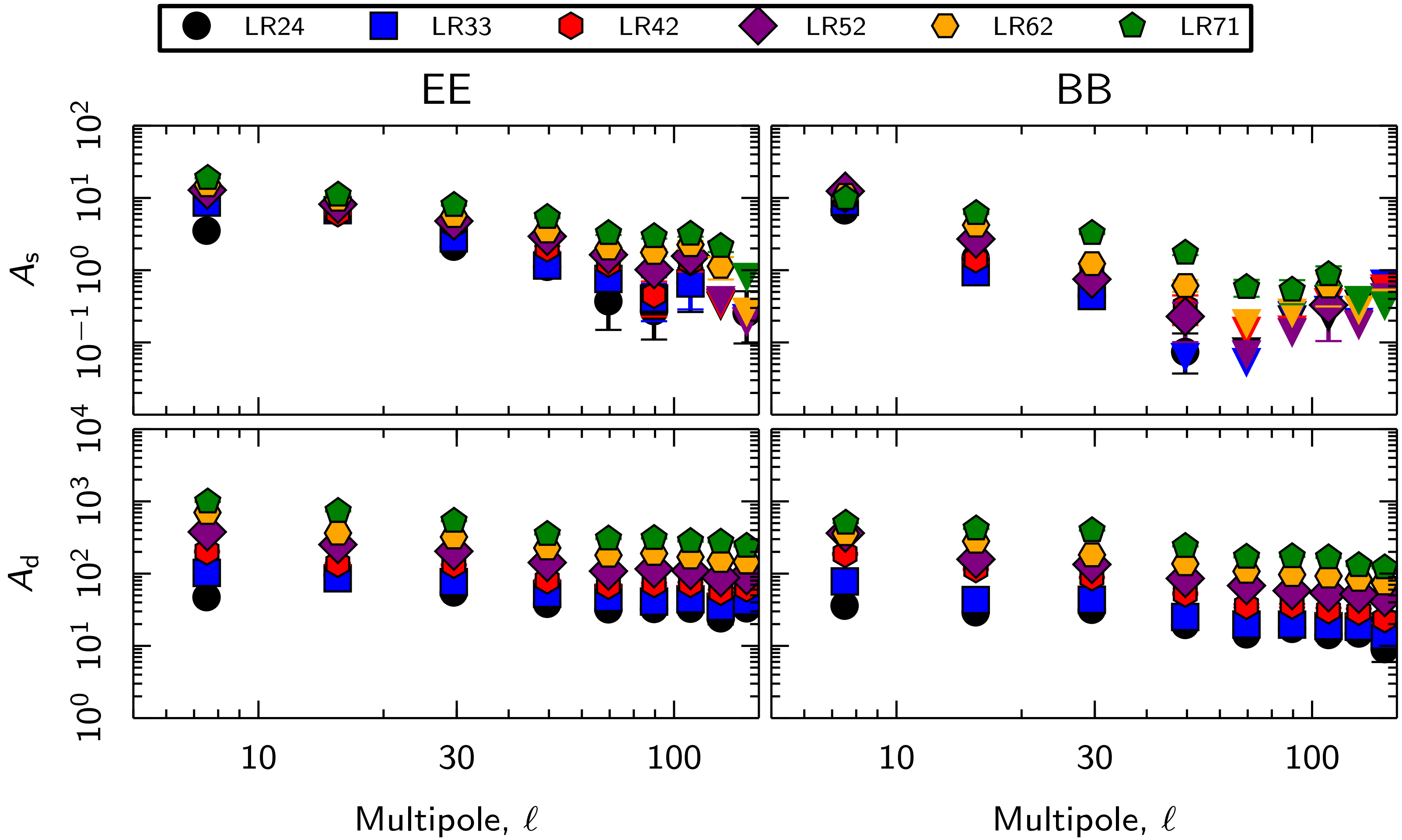

For B-modes, the synchrotron-to-dust ratio (A_s/A_d) is maximum at low multipoles and for the smallest sky region (LR24)

Comparison with CMB B-modes

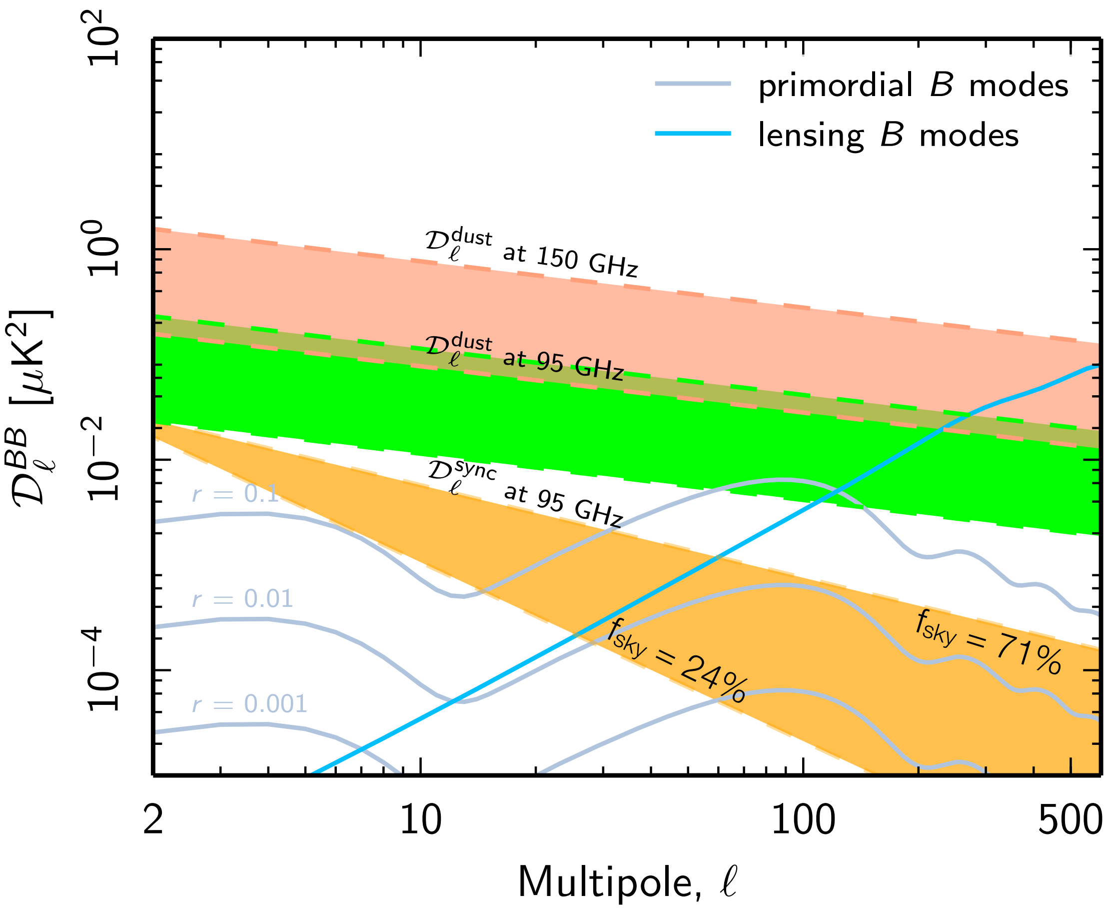

- *B*-modes dust and synchrotron power measured consistently for sky regions minimizing the dust foreground power for a given f_{sky}
- Synchrotron B-modes power decreases with ℓ more steeply than dust. The difference is the strongest for the cleanest sky region (LR24)
- In the cleanest sky regions, synchrotron is not a significant problem to reach a sensitivity limit on *r* of 10^{-2} at 95 GHz.

Frequency decorrelation

Two sky pixels, same I_{Dust} but different polarized intensity and polarization angle

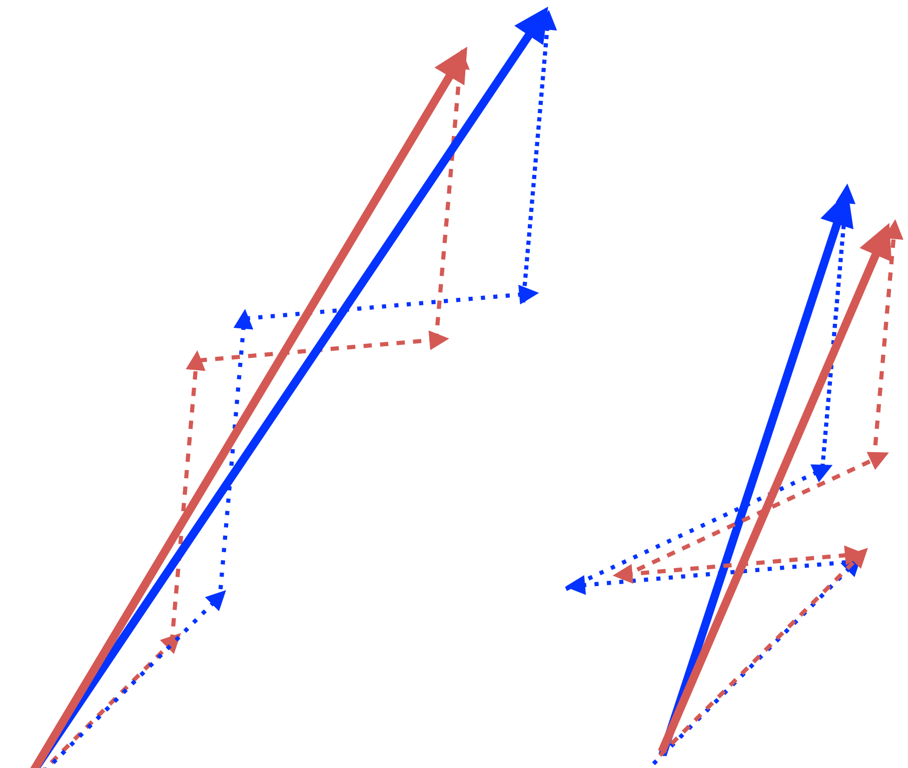

Sky pixel 1

Sky pixel 2

Frequencies ν_1 and ν_2

Statistically, dust polarization may be modeled as a random (oriented) walk in the Q,U plane with a small number of steps (Planck. Inter. XLII and L)

- The magnetic field orientation sets the direction of the step
- Dust polarized intensity sets the length
- Frequency decorrelation of the dust polarization signal between frequencies results from the correlation between the magnetic field, ISM structure and dust polarization properties.

➡ Both the polarized intensity and polarization angle change with frequency.

Simulating frequency decorrelation

Follow-up of HI-based dust polarization model (southern Galactic cap) from Ghosh et al. 2017

Different emission properties for the HI emission components

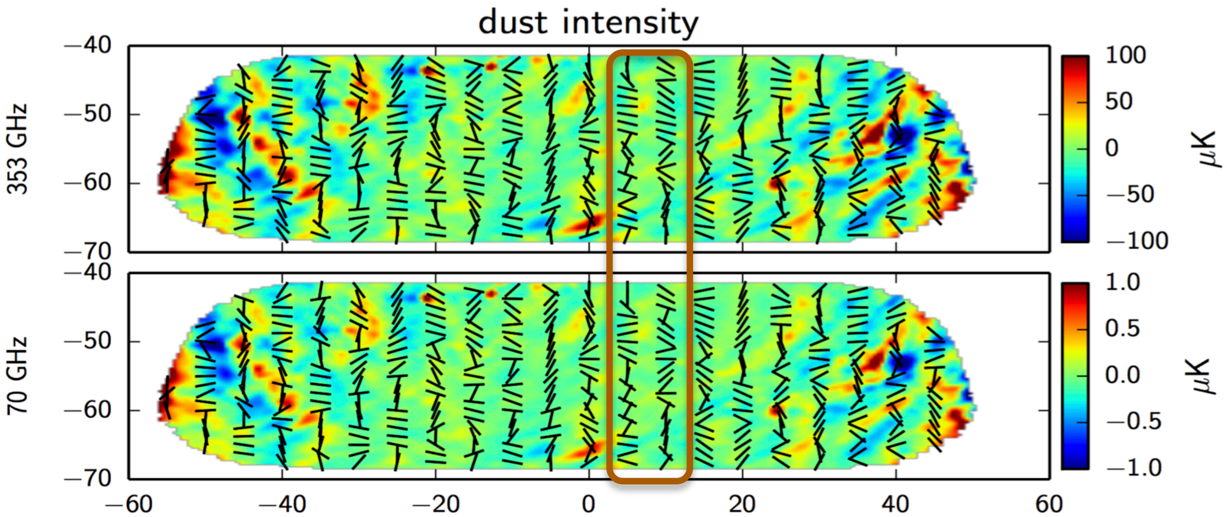

BICEP field, work in progress by T. Ghosh

Planck data analysis

Spectral correlation ratio:

$$\mathcal{R}_\ell^{BB} \equiv \frac{C_\ell^{BB}(217 \times 353)}{\sqrt{C_\ell^{BB}(353 \times 353)\, C_\ell^{BB}(217 \times 217)}}$$

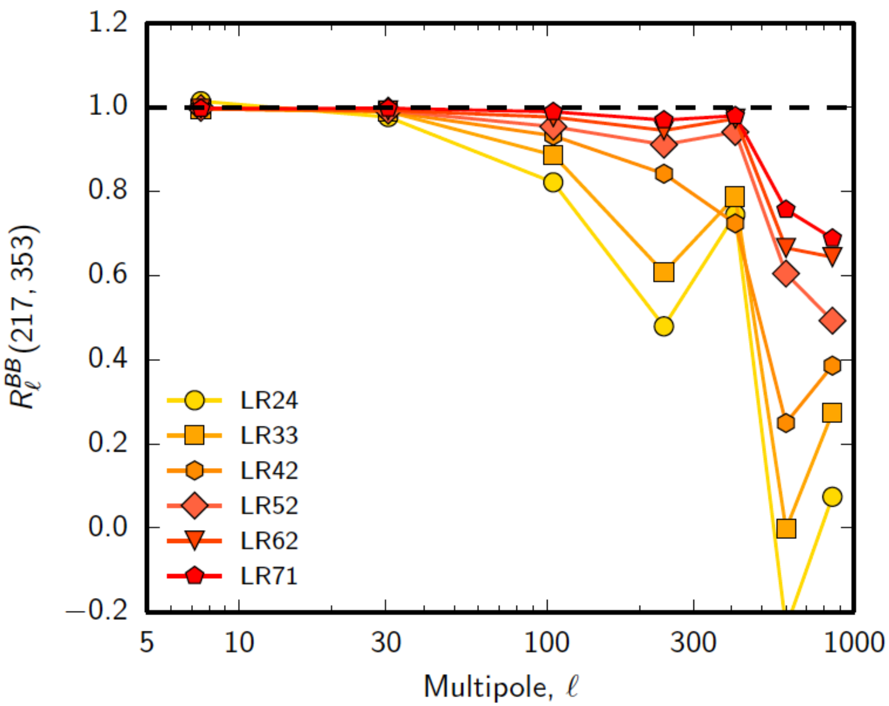

Planck Inter. LIV - 2017 Data

Result comparable to our earlier analysis on 2015 data (Planck Inter. L) suggesting significant decorrelation increasing towards the smallest (cleanest) sky regions, but the **statistical significance** of this result **was overstated,** as also pointed out by **Sheehy & Slosar (2017)** in their independent analysis

→ Chris Sheehy's talk

Histograms of $\mathcal{R}_\ell^{BB}$ for E2E simulations

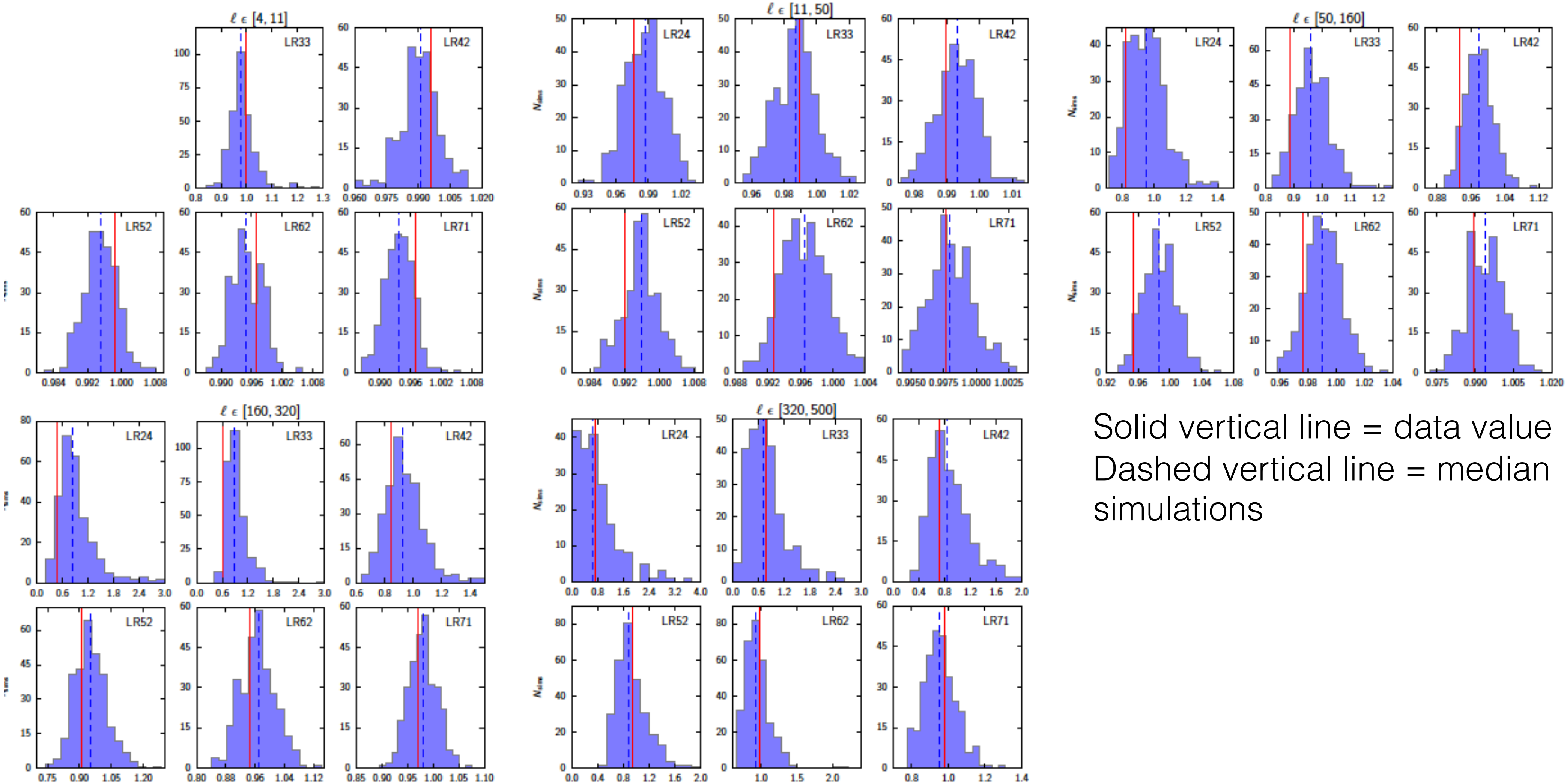

Solid vertical line = data value
Dashed vertical line = median simulations

Fig. B.1. Distribution of the correlation ratios $\mathcal{R}_\ell^{BB}$ on the six sky regions for each of the five ℓ-bins. The histograms are computed from the 300 E2E simulations using half-mission data splits. Histograms computed using odd-even surveys give similar results. The values derived from the data are displayed as vertical lines. The dashed lines represent the median value for the simulations.

Data versus E2E simulations

$$\mathcal{R}_\ell^{BB} \equiv \frac{C_\ell^{BB}(217 \times 353)}{\sqrt{C_\ell^{BB}(353 \times 353)\, C_\ell^{BB}(217 \times 217)}}$$

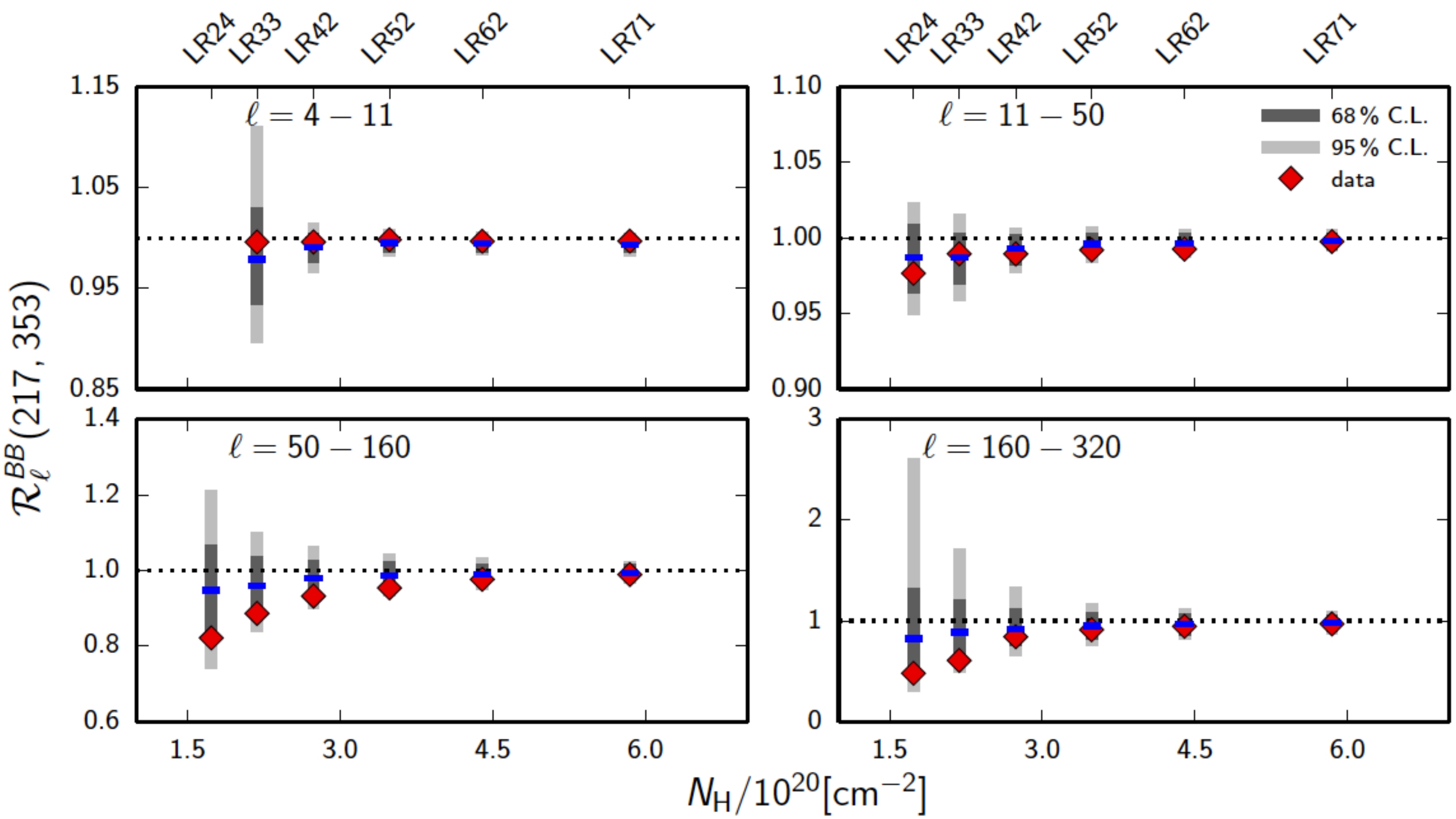

Confidence limits (68 and 95%) derived from E2E simulations

Planck Inter. LIV
2017 data

Correlation across regions

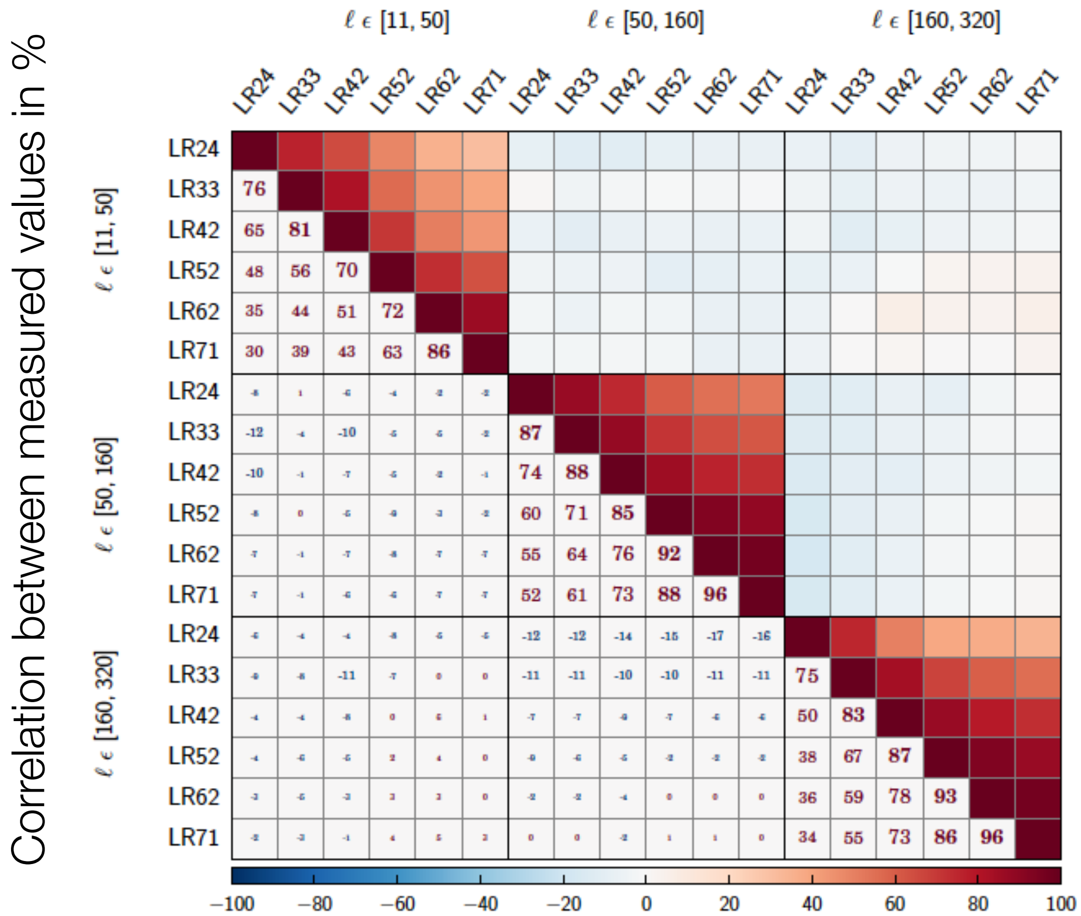

- Measurements for our set of nested sky regions, in a given multipole bin, are highly correlated
- As a result, **we overstated evidence for frequency decorrelation** when analyzing Planck 2015 data in Planck Inter. L

Multi-frequency approach in Tuhin Ghosh's talk